Atmos. Chem. Phys. Discuss., 14, 9951–9973, 2014
www.atmos-chem-phys-discuss.net/14/9951/2014/
doi:10.5194/acpd-14-9951-2014

spheric
emistry
Physics
Discussions
Open Access

On the hiatus in the acceleratio of tropical upwelling since the beg ning of the 21st century

J. Aschmann[1], **J. P. Burrows**[1], **C. Gebhardt**[1], **A. Rozanov**[1], **F** **nmel**[1], **M. Weber**[1], **and A. M. Thompson**[2]

[1]Institute of Environmental Physics, University of Bremen, Bremen, G y
[2]NASA/Goddard Space Flight Center, Greenbelt, MD, USA

Received: 19 March 2014 – Accepted: 7 April 2014 – Published: 17 A 14

Correspondence to: J. Aschmann (jan.aschmann@iup.physik.uni-brei e)

Published by Copernicus Publications on behalf of the European Geo es Union.

Abstract

Chemistry–climate models predict an acceleration of the upwelling branch of the Brewer–Dobson circulation as a consequence of increasing global surface temperatures, resulting from elevated levels of atmospheric greenhouse gases. The observed decrease of ozone in the tropical lower stratosphere during the last decades of the 20th century is consistent with the anticipated acceleration of upwelling. However, more recent satellite observations of ozone reveal that this decrease has unexpectedly stopped in the first decade of the 21st century, challenging the implicit assumption of a continuous acceleration of tropical upwelling. In this study we use three decades of chemistry-transport-model simulations (1980–2013) to investigate this phenomenon and resolve this apparent contradiction. Our model reproduces the observed tropical lower stratosphere ozone record, showing a significant decrease in the early period followed by a statistically robust trend-change after 2002. We demonstrate that this trend-change is correlated with corresponding changes in the vertical transport and conclude that a hiatus in the acceleration of tropical upwelling occurred during the last decade.

1 Introduction

The issue of whether the large-scale Brewer–Dobson Circulation (BDC) has strengthened in the recent past, as a result of anthropogenic activity, has been raised (Oman et al., 2009; Butchart et al., 2010; Randel and Jensen, 2013). Recent chemistry-climate model (CCM) simulations predict an increase of resolved wave activity and orographic gravity wave drag resulting from increasing sea surface temperatures (Garcia and Randel, 2008; Oman et al., 2009; Waugh et al., 2009; Butchart et al., 2010; Garny et al., 2011). This strengthens the upwelling branch of the BDC, commonly referred to as the tropical upwelling. In comparison, the behaviour of the observations is ambiguous. The long-term cooling of the tropical lower stratosphere (LS, about 17–21 km; Thompson and Solomon, 2005; Young et al., 2012) and the observed weakening of the stratospheric quasi-biennial oscillation (QBO; Kawatani and Hamilton, 2013) are consistent with the predicted increase of upwelling. On the other hand, the mean residence time of air parcels in the stratosphere (age of air) inferred from sulfur hexafluoride (SF_6) measurements is inconsistent with an overall acceleration of the BDC (Engel et al., 2009; Stiller et al., 2012). They indicate no significant changes or even deceleration of the vertical transport in the middle stratosphere. To reconcile the observed discrepancies it has been argued that the individual branches of the BDC are evolving differently, i.e. an increase in tropical upwelling does not necessarily imply an acceleration of the overall circulation (Bönisch et al., 2011; Diallo et al., 2012; Lin and Fu, 2013).

Ozone (O_3) is a sensitive proxy for vertical transport in the tropical LS (Randel et al., 2006; Waugh et al., 2009; Randel and Thompson, 2011; Polvani and Solomon, 2012). Its local mixing ratio is considered to result from a stationary state involving production by oxygen (O_2) photo-dissociation and a steady influx of O_3-poor tropospheric air from below (Avallone and Prather, 1996; Waugh et al., 2009; Meul et al., 2014). Meridional mixing from higher latitudes is a secondary effect that contributes to the seasonality in the O_3 mixing ratios (Ploeger et al., 2012). Several studies have reported a negative trend of O_3 in the tropical LS in the range of −(3–6) % per decade, consistent with the CCM predicted increase of tropical upwelling (Randel and Thompson, 2011; Sioris et al., 2014; Bourassa et al., 2014). In contrast, more recent O_3 observations from various satellite instruments indicate no statistically significant decrease of LS O_3 since the beginning of the 21st century (Kyrölä et al., 2013; Eckert et al., 2014; Gebhardt et al., 2014).

Stimulated by the need to explain the unusual linear trends revealed from the vertical profile of O_3 retrieved from SCIAMACHY[1] we use three decades of O_3 observations and simulations to investigate this phenomenon. Section 2 describes the observations, model and regression analysis used in this study. The results are discussed in Sect. 3.

[1]First reported at the Quadrennial Ozone Symposium 2012 Toronto, 27–31 August 2012 and published in Gebhardt et al. (2014).

2 Data and analysis

2.1 Observations

For a quantitative analysis of tropical upwelling, we use combined O_3 observations from satellite instruments and sondes. The earlier decades (1985–2005) are covered by the ERBS/SAGE II instrument (McCormick et al., 1989), providing O_3 profiles based on solar occultation measurements. Due to its viewing geometry, the vertical resolution of the profiles is high (1 km, range 15–50 km), although the horizontal sampling is relatively sparse (global coverage in 1 month). Here we use version 7.0 of the data (Damadeo et al., 2013), screened for cloud and aerosol contaminated profiles as suggested by Wang et al. (2002). Two years of data after June 1991 has been omitted due to contamination by the eruption of Mt. Pinatubo. For the last decade (2002–2012), we use O_3 observations from ENVISAT/SCIAMACHY (Burrows et al., 1995) based on limb geometry (retrieval version 2.9; Sonkaew et al., 2009). The vertical resolution is about 3–4 km over an altitude range of 10–75 km; global coverage is achieved every 6 days. Data from both instruments has been binned into monthly samples on a uniform horizontal and vertical grid (15° lon. × 5° lat. × 1 km). To minimise sampling issues and taking into account the differences in horizontal and vertical resolution of the instruments, any further analysis is based on partial columns of O_3 between 17–21 km and 20° N–20° S, similar to the approach of Randel and Thompson (2011).

The satellite data is augmented by an ensemble of tropical sonde measurements from the Southern Hemisphere Additional Ozonesondes network (SHADOZ; 1998–2013; Thompson et al., 2003, 2012). We use 10 sites located in the tropics with long and continuous records. The selected stations along with their temporal coverage and mean value are listed in Table 1. Typically there are 2–4 observations per month for each SHADOZ station, which provide O_3 profiles in a considerable higher vertical resolution (50–100 m) compared to the satellite instruments. As there is a high degree of longitudinal symmetry in the stratospheric ozone profiles (Thompson et al., 2003), we average the individual records to obtain a representative mean for the tropics.

ACPD
14, 9951–9973, 2014

Hiatus in the acceleration of tropical upwelling

J. Aschmann et al.

2.2 Model

To obtain a consistent timeseries of LS O_3 of the last decades for direct comparison with observations, we conducted a 33-year simulation with the Bremen three-dimensional chemistry-transport-model (B3DCTM; Sinnhuber et al., 2003; Aschmann et al., 2009; Aschmann and Sinnhuber, 2013). The current version of the model has a horizontal resolution of 3.75° lon. × 2.5° lat. and covers the vertical domain from the surface up to approximately 55 km using a hybrid $\sigma - \theta$ coordinate system (e.g., Chipperfield, 2006). The vertical resolution in the tropical LS is about 600 m. The model is driven by 6-hourly input of European Centre for Medium-range Weather Forecast (ECMWF) Era-Interim (EI; Dee et al., 2011) reanalysis data. Vertical transport in the purely isentropic domain (above ≈ 16 km in the tropics) is prescribed by EI all-sky heating rates. The B3DCTM incorporates a comprehensive chemistry scheme originally based on the chemistry part of the SLIMCAT model (Chipperfield, 1999), covering all relevant photochemical reactions for stratospheric O_3 chemistry. Reaction rates and absorption cross sections are taken from the Jet Propulsion Laboratory recommendations (Sander et al., 2011). To avoid initialisation artefacts, the model has been run with replicated input data to reach steady state before starting the actual integration from January 1979 to October 2013.

2.3 Regression

The multivariate regression analysis used throughout this study is based on Reinsel et al. (2002) with Y_t as the monthly mean variable to be fitted:

$$
\begin{aligned}
Y_t = {} & \mu + S_t + \omega_1 X_{1t} + \omega_2 X_{2t} + \mathrm{QBO}_t + \mathrm{ENSO}_t \\
& + \mathrm{SC}_t + N_t
\end{aligned}
\tag{1}
$$

Here, μ is the baseline constant, S_t a seasonal component, $\omega_{1,2}$ are the trend coefficients with $X_{1,2t}$ as linear trend functions and N_t represents the unexplained noise.

ACPD
14, 9951–9973, 2014

Note that in contrast to previous studies, which examined LS O_3 (Randel and Thompson, 2011; Sioris et al., 2014), our regression model assumes two linear components, which account for a possible change of trend. Here, ϖ_1 is the linear trend up to a specified inflexion date T_0. After T_0, the new linear trend ϖ comprises the sum of the earlier trend ϖ_1 and the trend-change component ϖ_2. The additional regression terms are QBO_t for QBO, $ENSO_t$ for the El Niño Southern Oscillation (ENSO) and SC_t for solar cycle. The QBO proxy consists of the QBO.U30 and QBO.U50 (zonal wind 30/50 hPa) from the NOAA Climate Prediction Center[2], the ENSO proxy is represented by the Multivariate ENSO Index (MEI) from the NOAA Earth System Research Laboratory[3] (Wolter and Timlin, 2011) lagged by two months and the solar cycle by the Bremen composite Mg II index[4] (Snow et al., 2014).

Assuming first order autocorrelation noise (AR(1) model), as commonly used in the regression of O_3 timeseries (e.g., Reinsel et al., 2002; Jones et al., 2009; Sioris et al., 2014), the corresponding errors for the trend components calculate as

$$\sigma_{\varpi_1} \approx \frac{\sigma_N}{n^{3/2}} \sqrt{\frac{1+\phi}{1-\phi}} \tag{2}$$

$$\sigma_{\varpi_2} \approx \frac{\sigma_N}{2} \sqrt{\frac{1+\phi}{1-\phi}} \left(\frac{n}{n_0 n_1}\right)^{3/2} \tag{3}$$

$$\sigma_{\varpi} \approx \frac{\sigma_N}{n_1^{3/2}} \sqrt{\frac{1+\phi}{1-\phi}} \sqrt{\frac{n_0+4n_1}{4n}}. \tag{4}$$

[2]www.cpc.ncep.noaa.gov/data/indices/
[3]www.esrl.noaa.gov/psd/enso/mei/
[4]www.iup.uni-bremen.de/gome/solar/MgII_composite.dat

Discussion Paper | Discussion Paper | Discussion Paper | Discussion Paper |
ACPD
14, 9951–9973, 2014
Hiatus in the acceleration of tropical upwelling
J. Aschmann et al.

Here, σ_N is the standard error of the fit residuals, n_0, n_1 are the numbers of years of data before and after the trend-change, respectively, with $n = n_0 + n_1$. ϕ represents the autocorrelation of the residuals with a time lag of 1 month.

The choice of the inflexion year T_0 is essentially a free parameter in the regression analysis. Figure 1 illustrates the impact of the choice of T_0 on the regression of modelled LS O_3 columns and EI upward mass flux (as discussed below in Sect. 3). A 2σ-significant trend-change (ϖ_2) is obtained for a wide range of possible inflexion years (marked by red circles). Therefore we use a χ^2 test based on the fit residuals, similar to the approach described by Jones et al. (2009), to identify the most probable inflexion year. We find a clear minimum in the χ^2 values close to 2002 and consequently select this year as the turning point in the trend analysis.

3 Results and discussion

3.1 Lower stratosphere ozone column

Figure 2 presents tropical LS O_3 column anomalies (20° N–20° S, 17–21 km) from measurements and the simulation. The agreement between model and observations is good, except for a small high-bias relative to the earlier SAGE II data (1985–1990) of approximately 1 DU: correlation coefficients are 0.65 between modelled and observed datasets.

A decline of O_3 is evident in the tropical LS during the first two decades (1980–2002), both in the observed and modelled timeseries. This is consistent with an increase of tropical upwelling during this period. However, this trend vanishes in the third decade (2002–2013). Figure 3a and b illustrates the results from the regression analysis of the modelled timeseries showing the fit function and the corresponding residuals, respectively. The linear trend amounts to -8.1 ± 0.9 % per decade (ϖ_1) in the pre-2002 period and 0.1 ± 3.3 % per decade (ϖ) for the remaining years. The resulting trend-change of

ACPD
14, 9951–9973, 2014

8.2 % per decade (ϖ_2) is statistically significant within the 95 % confidence interval (i.e. $\varpi_2 > 2\sigma_{\varpi}$).

To apply our analysis to the observational data we merge the available datasets (SAGE II–SCIAMACHY; SAGE II–SHADOZ). In either case, the correlation between LS O_3 partial columns exceeds 0.8 in the overlap period and the bias is generally lower than 2 %. Considering the good agreement between the observations it is reasonable to combine them into a continuous timeseries. We adopt the method described in Randel and Thompson (2011) and simply join the two individual timeseries and average the overlap period. When we apply the regression to the combined SAGE II–SCIAMACHY timeseries, we calculate a trend of -3.9 ± 0.5 % per decade (ϖ_1) for the pre-2002 period, consistent with the range of $-(3–6)$ % per decade given by earlier studies (Fig. 3c and d; Randel and Thompson, 2011; Sioris et al., 2014; Bourassa et al., 2014). The discrepancy between model and observations for the pre-2002 trend is likely caused by the O_3 high-bias between 1985–1990, mentioned above, and the possibly overestimated vertical transport velocity in the EI dataset (Ploeger et al., 2012; Diallo et al., 2012), which is discussed below in more detail. After 2002 the trend is 0.5 ± 1.5 % per decade (ϖ), yielding a statistically significant trend-change of 4.4 % per decade (ϖ_2). We obtain similar values (-3.6 ± 0.5, 0.4 ± 1.4 % per decade for ϖ_1, ϖ) if we use the SHADOZ data instead of SCIAMACHY in the combined dataset. Consequently, both observational and model data show that the decrease of LS O_3 has effectively stopped since about 2002. This is in qualitative agreement with those studies, which focus solely on the most recent observational record of O_3, although the differences in utilised regression models and timeseries length make a direct comparison difficult. Gebhardt et al. (2014) compared several satellite instruments and report consistently positive trends of tropical O_3 between 17–21 km, ranging from about 2 (OSIRIS), 4 (SCIAMACHY) up to 14 % per decade (MLS), covering the years 2004–2012. Eckert et al. (2014) find a slightly positive trend of 0–1 % per decade in the same region in MIPAS observations (2002–2012).

ACPD
14, 9951–9973, 2014

Local chemical effects can be largely ruled out as explanation for the detected trend-change of LS O_3. As stated above, O_3 abundance in the tropical LS is mainly determined by vertical transport and O_2 photolysis (Avallone and Prather, 1996; Waugh et al., 2009; Meul et al., 2014). O_3-destroying catalytic species are scarce in the tropical LS, therefore the phase-out of ozone-depleting substances (ODS), and the associated recovery (e.g., World Meteorological Organization, 2011), has no direct impact on O_3 concentrations in this region. However, some studies point out a possible indirect relationship between ODS-related polar O_3 depletion and tropical LS O_3 by dynamical coupling (Waugh et al., 2009; Oman et al., 2009). Meul et al. (2014) predict an increase of photolytic O_3 production as a result from long-term changes in the overhead O_3 column. Furthermore, an increase in odd nitrogen (NO_x) might lead to additional O_3 production. However, neither process is sufficient to explain a short-term trend-change. Overall the most probable explanation of the observed behaviour is that changes in dynamics must be involved.

3.2 Tropical upwelling

Some studies point out that the increase of tropical upwelling may be compensated by an, as yet, unexplained weakening or shifting of tropical mixing barriers (Stiller et al., 2012; Eckert et al., 2014). However, it is also possible that the increase of tropical upwelling itself has ceased. To investigate this hypothesis, we analyse tropical upwelling in the EI reanalysis that drives our model. A typical representative quantity for the tropical upwelling is the upward mass flux at 70 hPa ($\approx$ 18.5 km in the tropics; Butchart et al., 2010; Seviour et al., 2012). A recent study assessing the upward mass flux in EI found a negative trend of −5 % per decade for the years 1989–2009, based on EI kinematic vertical winds (Seviour et al., 2012). This is in contradiction with the results of current CCM, which predict an increase of upwelling of about 2.0 % per decade (ensemble mean; Butchart et al., 2010). The quality of stratospheric vertical transport in EI improves considerably, when diabatic heating rates are used instead of the kinematic wind. Although tending to overestimate the tropical ascent (Ploeger et al., 2012), the

ACPD
14, 9951–9973, 2014

diabatic representation of vertical transport yields more realistic estimates of stratospheric age of air in comparison to the kinematic approach (Diallo et al., 2012) and is also less dispersive (Ploeger et al., 2011).

Figure 4 shows the tropical LS EI all-sky heating rates (20° N–20° S, 17–21 km; panel a), which are used to drive the vertical transport in our isentropic model, and the corresponding EI upward mass flux at 70 hPa (panel c). The upward mass flux is the integral of the residual vertical velocity w^* between turnaround latitudes as described in Seviour et al. (2012). In turn, w^* is calculated from the EI heating rates using the iterative algorithm described by Solomon et al. (1986). Applying the regression analysis to the upward mass flux yields a positive trend of 3.3 ± 0.7 % per decade for the pre-2002 period (Fig. 4d). This value is consistent with the CCM results (2.0 % per decade) although somewhat high-biased, reflecting the overestimation of vertical transport mentioned above. After 2002, however, there is a statistically significant trend-change around 2002 leading to a negative trend of -2.3 ± 2.5 % per decade mirroring the trend-change in the LS O_3 timeseries. We find significant anti-correlation between LS O_3 anomalies with either heating rates (−0.83), or upward mass flux anomalies (−0.55). Taking into account the known sensitivity of LS O_3 to vertical transport, we conclude that the observed trend-change in O_3 is primarily a consequence of the simultaneous trend-change in tropical upwelling.

4 Conclusions

In summary, we find a negative trend of tropical LS O_3 in observations and model before 2002, associated with a positive trend in tropical upwelling from the EI dataset based upon diabatic heating calculation. This finding is consistent with earlier studies (Butchart et al., 2010; Randel and Thompson, 2011). We also find an unexpected hiatus of the negative trend in LS O_3 during the last decade. We explain this behaviour by the change of tropical upwelling evident in the EI dataset. This change may be a consequence of the unexpected La-Niña-like cooling of the equatorial Eastern Pacific since the beginning of the 21st century (Meehl et al., 2011). The latter has a significant impact on global surface temperatures (Kosaka and Xie, 2013) and ultimately, by dynamical coupling, on tropical upwelling (Oman et al., 2009; Butchart et al., 2010; Garny et al., 2011). Recent studies describe the associated circulation changes (England et al., 2014) and their impact on tropospheric O_3 (Lin et al., 2014). In contrast to current unconstrained CCM, which generally do not predict this exceptional heat uptake by the equatorial Eastern Pacific (Kosaka and Xie, 2013; England et al., 2014), this feature can be clearly observed in the data-assimilated EI dataset (Fig. 5). In conclusion the accuracy of our predictions of future BDC development and its consequences for stratospheric O_3 critically depends on our understanding of the ocean-atmosphere interaction.

Acknowledgements. This study has been funded in part by the University and State of Bremen, the DFG Research Unit 1095 Stratospheric Change and its Role for Climate Prediction, SHARP, and the German Federal Ministry of Education and Research, research project Role of the middle atmosphere in climate (ROMIC). SHADOZ, the Southern Hemisphere Additional Ozonesondes network, is funded by NASA's Upper Atmosphere Research Program.

References

Aschmann, J. and Sinnhuber, B.-M.: Contribution of very short-lived substances to stratospheric bromine loading: uncertainties and constraints, Atmos. Chem. Phys., 13, 1203–1219, doi:10.5194/acp-13-1203-2013, 2013. 9955

Aschmann, J., Sinnhuber, B.-M., Atlas, E. L., and Schauffler, S. M.: Modeling the transport of very short-lived substances into the tropical upper troposphere and lower stratosphere, Atmos. Chem. Phys., 9, 9237–9247, doi:10.5194/acp-9-9237-2009, 2009. 9955

Avallone, L. M. and Prather, M. J.: Photochemical evolution of ozone in the lower tropical stratosphere, J. Geophys. Res.-Atmos., 101, 1457–1461, doi:10.1029/95JD03010, 1996. 9953, 9959

Bönisch, H., Engel, A., Birner, Th., Hoor, P., Tarasick, D. W., and Ray, E. A.: On the structural changes in the Brewer-Dobson circulation after 2000, Atmos. Chem. Phys., 11, 3937–3948, doi:10.5194/acp-11-3937-2011, 2011. 9953

Bourassa, A. E., Degenstein, D. A., Randel, W. J., Zawodny, J. M., Kyrölä, E., McLinden, C. A., Sioris, C. E., and Roth, C. Z.: Trends in stratospheric ozone derived from merged SAGE II and Odin-OSIRIS satellite observations, Atmos. Chem. Phys. Discuss., 14, 7113–7140, doi:10.5194/acpd-14-7113-2014, 2014. 9953, 9958

Burrows, J., Hölzle, E., Goede, A., Visser, H., and Fricke, W.: SCIAMACHY – scanning imaging absorption spectrometer for atmospheric chartography, Acta Astronaut., 35, 445–451, doi:10.1016/0094-5765(94)00278-T, 1995. 9954

Butchart, N., Cionni, I., Eyring, V., Shepherd, T. G., Waugh, D. W., Akiyoshi, H., Austin, J., Bruehl, C., Chipperfield, M. P., Cordero, E., Dameris, M., Deckert, R., Dhomse, S., Frith, S. M., Garcia, R. R., Gettelman, A., Giorgetta, M. A., Kinnison, D. E., Li, F., Mancini, E., McLandress, C., Pawson, S., Pitari, G., Plummer, D. A., Rozanov, E., Sassi, F., Scinocca, J. F., Shibata, K., Steil, B., and Tian, W.: Chemistry-climate model simulations of twenty-first century stratospheric climate and circulation changes, J. Climate, 23, 5349–5374, doi:10.1175/2010JCLI3404.1, 2010. 9952, 9959, 9960, 9961

Chipperfield, M. P.: Multiannual simulations with a three-dimensional chemical transport model, J. Geophys. Res.-Atmos., 104, 1781–1805, 1999. 9955

Chipperfield, M. P.: New version of the TOMCAT/SLIMCAT off-line chemical transport model: intercomparison of stratospheric tracer experiments, Q. J. Roy. Meteor. Soc., 132, 1179–1203, doi:10.1256/qj.05.51, 2006. 9955

Damadeo, R. P., Zawodny, J. M., Thomason, L. W., and Iyer, N.: SAGE version 7.0 algorithm: application to SAGE II, Atmos. Meas. Tech., 6, 3539–3561, doi:10.5194/amt-6-3539-2013, 2013. 9954

Dee, D. P., Uppala, S. M., Simmons, A. J., Berrisford, P., Poli, P., Kobayashi, S., Andrae, U., Balmaseda, M. A., Balsamo, G., Bauer, P., Bechtold, P., Beljaars, A. C. M., van de Berg, L., Bidlot, J., Bormann, N., Delsol, C., Dragani, R., Fuentes, M., Geer, A. J., Haimberger, L., Healy, S. B., Hersbach, H., Hólm, E. V., Isaksen, L., Kållberg, P., Köhler, M., Matricardi, M., McNally, A. P., Monge-Sanz, B. M., Morcrette, J.-J., Park, B.-K., Peubey, C., de Rosnay, P., Tavolato, C., Thépaut, J.-N., and Vitart, F.: The ERA-Interim reanalysis: configuration and performance of the data assimilation system, Q. J. Roy. Meteor. Soc., 137, 553–597, doi:10.1002/qj.828, 2011. 9955

ACPD
14, 9951–9973, 2014

Hiatus in the acceleration of tropical upwelling

J. Aschmann et al.

Diallo, M., Legras, B., and Chédin, A.: Age of stratospheric air in the ERA-Interim, Atmos. Chem. Phys., 12, 12133–12154, doi:10.5194/acp-12-12133-2012, 2012. 9953, 9958, 9960

Eckert, E., von Clarmann, T., Kiefer, M., Stiller, G. P., Lossow, S., Glatthor, N., Degenstein, D. A., Froidevaux, L., Godin-Beekmann, S., Leblanc, T., McDermid, S., Pastel, M., Steinbrecht, W., Swart, D. P. J., Walker, K. A., and Bernath, P. F.: Drift-corrected trends and periodic variations in MIPAS IMK/IAA ozone measurements, Atmos. Chem. Phys., 14, 2571–2589, doi:10.5194/acp-14-2571-2014, 2014. 9953, 9958, 9959

Engel, A., Moebius, T., Bönisch, H., Schmidt, U., Heinz, R., Levin, I., Atlas, E., Aoki, S., Nakazawa, T., Sugawara, S., Moore, F., Hurst, D., Elkins, J., Schauffler, S., Andrews, A., and Boering, K.: Age of stratospheric air unchanged within uncertainties over the past 30 years, Nat. Geosci., 2, 28–31, doi:10.1038/NGEO388, 2009. 9953

England, M. H., McGregor, S., Spence, P., Meehl, G. A., Timmermann, A., Cai, W., Gupta, A. S., McPhaden, M. J., Purich, A., and Santoso, A.: Recent intensification of wind-driven circulation in the Pacific and the ongoing warming hiatus, Nat. Clim. Change, 4, 222–227, doi:10.1038/nclimate2106, 2014. 9961

Garcia, R. R. and Randel, W. J.: Acceleration of the Brewer–Dobson circulation due to increases in greenhouse gases, J. Atmos. Sci., 65, 2731–2739, doi:10.1175/2008JAS2712.1, 2008. 9952

Garny, H., Dameris, M., Randel, W., Bodeker, G. E., and Deckert, R.: Dynamically forced increase of tropical upwelling in the lower stratosphere, J. Atmos. Sci., 68, 1214–1233, doi:10.1175/2011JAS3701.1, 2011. 9952, 9961

Gebhardt, C., Rozanov, A., Hommel, R., Weber, M., Bovensmann, H., Burrows, J. P., Degenstein, D., Froidevaux, L., and Thompson, A. M.: Stratospheric ozone trends and variability as seen by SCIAMACHY from 2002 to 2012, Atmos. Chem. Phys., 14, 831–846, doi:10.5194/acp-14-831-2014, 2014. 9953, 9958

Jones, A., Urban, J., Murtagh, D. P., Eriksson, P., Brohede, S., Haley, C., Degenstein, D., Bourassa, A., von Savigny, C., Sonkaew, T., Rozanov, A., Bovensmann, H., and Burrows, J.: Evolution of stratospheric ozone and water vapour time series studied with satellite measurements, Atmos. Chem. Phys., 9, 6055–6075, doi:10.5194/acp-9-6055-2009, 2009. 9956, 9957

Kawatani, Y. and Hamilton, K.: Weakened stratospheric quasibiennial oscillation driven by increased tropical mean upwelling, Nature, 497, 478–481, doi:10.1038/nature12140, 2013. 9953

ACPD

14, 9951–9973, 2014

Hiatus in the acceleration of tropical upwelling

J. Aschmann et al.

Kosaka, Y. and Xie, S.-P.: Recent global-warming hiatus tied to equatorial Pacific surface cooling, Nature, 501, 403–407, doi:10.1038/nature12534, 2013. 9961, 9973

Kyrölä, E., Laine, M., Sofieva, V., Tamminen, J., Päivärinta, S.-M., Tukiainen, S., Zawodny, J., and Thomason, L.: Combined SAGE II–GOMOS ozone profile data set for 1984–2011 and trend analysis of the vertical distribution of ozone, Atmos. Chem. Phys., 13, 10645–10658, doi:10.5194/acp-13-10645-2013, 2013. 9953

Lin, M., Horowitz, L. W., Oltmans, S. J., Fiore, A. M., and Fan, S.: Tropospheric ozone trends at Mauna Loa Observatory tied to decadal climate variability, Nat. Geosci., 7, 136–143, doi:10.1038/ngeo2066, 2014. 9961

Lin, P. and Fu, Q.: Changes in various branches of the Brewer–Dobson circulation from an ensemble of chemistry climate models, J. Geophys. Res.-Atmos., 118, 73–84, doi:10.1029/2012JD018813, 2013. 9953

McCormick, M., Zawodny, J., Veiga, R., Larsen, J., and Wang, P.: An overview of SAGE-I and SAGE-II ozone measurements, Planet. Space Sci., 37, 1567–1586, doi:10.1016/0032-0633(89)90146-3, 1989. 9954

Meehl, G. A., Arblaster, J. M., Fasullo, J. T., Hu, A., and Trenberth, K. E.: Model-based evidence of deep-ocean heat uptake during surface-temperature hiatus periods, Nat. Clim. Change, 1, 360–364, doi:10.1038/NCLIMATE1229, 2011. 9961

Meul, S., Langematz, U., Oberländer, S., Garny, H., and Jöckel, P.: Chemical contribution to future tropical ozone change in the lower stratosphere, Atmos. Chem. Phys., 14, 2959–2971, doi:10.5194/acp-14-2959-2014, 2014. 9953, 9959

Oman, L., Waugh, D. W., Pawson, S., Stolarski, R. S., and Newman, P. A.: On the influence of anthropogenic forcings on changes in the stratospheric mean age, J. Geophys. Res.-Atmos., 114, D03105, doi:10.1029/2008JD010378, 2009. 9952, 9959, 9961

Ploeger, F., Fueglistaler, S., Grooß, J.-U., Günther, G., Konopka, P., Liu, Y.S., Müller, R., Ravegnani, F., Schiller, C., Ulanovski, A., and Riese, M.: Insight from ozone and water vapour on transport in the tropical tropopause layer (TTL), Atmos. Chem. Phys., 11, 407–419, doi:10.5194/acp-11-407-2011, 2011. 9960

Ploeger, F., Konopka, P., Mueller, R., Fueglistaler, S., Schmidt, T., Manners, J. C., Grooss, J.-U., Guenther, G., Forster, P. M., and Riese, M.: Horizontal transport affecting trace gas seasonality in the Tropical Tropopause Layer (TTL), J. Geophys. Res.-Atmos., 117, D09303, doi:10.1029/2011JD017267, 2012. 9953, 9958, 9959

Polvani, L. M. and Solomon, S.: The signature of ozone depletion on tropical temperature trends, as revealed by their seasonal cycle in model integrations with single forcings, J. Geophys. Res.-Atmos., 117, D17102, doi:10.1029/2012JD017719, 2012. 9953

Randel, W. J. and Jensen, E. J.: Physical processes in the tropical tropopause layer and their roles in a changing climate, Nat. Geosci., 6, 169–176, doi:10.1038/ngeo1733, 2013. 9952

Randel, W. J. and Thompson, A. M.: Interannual variability and trends in tropical ozone derived from SAGE II satellite data and SHADOZ ozonesondes, J. Geophys. Res.-Atmos., 116, D07303, doi:10.1029/2010JD015195, 2011. 9953, 9954, 9956, 9958, 9960

Randel, W. J., Wu, F., Voemel, H., Nedoluha, G. E., and Forster, P.: Decreases in stratospheric water vapor after 2001: links to changes in the tropical tropopause and the Brewer–Dobson circulation, J. Geophys. Res.-Atmos., 111, D12312, doi:10.1029/2005JD006744, 2006. 9953

Reinsel, G. C., Weatherhead, E. C., Tiao, G. C., Miller, A. J., Nagatani, R. M., Wuebbles, D. J., and Flynn, L. E.: On detection of turnaround and recovery in trend for ozone, J. Geophys. Res.-Atmos., 107, 4078, doi:10.1029/2001JD000500, 2002. 9955, 9956

Sander, S. P., Abbatt, J., Barker, J. R., Burkholder, J. B., Friedl, R. R., Golden, D. M., Huie, R. E., Kolb, C. E., Kurylo, M. J., Moortgat, G. K., Orkin, V. L., and Wine, P. H.: Chemical Kinetics and Photochemical Data for Use in Atmospheric Studies: Evaluation No. 17, JPL Publ. 10-6, Jet Propul. Lab., Pasadena, CA, 2011. 9955

Seviour, W. J. M., Butchart, N., and Hardiman, S. C.: The Brewer–Dobson circulation inferred from ERA-Interim, Q. J. Roy. Meteor. Soc., 138, 878–888, doi:10.1002/qj.966, 2012. 9959, 9960

Sinnhuber, B.-M., Weber, M., Amankwah, A., and Burrows, J. P.: Total ozone during the unusual Antarctic winter of 2002, Geophys. Res. Lett., 30, 1580, doi:10.1029/2002GL016798, 2003. 9955

Sioris, C. E., McLinden, C. A., Fioletov, V. E., Adams, C., Zawodny, J. M., Bourassa, A. E., Roth, C. Z., and Degenstein, D. A.: Trend and variability in ozone in the tropical lower stratosphere over 2.5 solar cycles observed by SAGE II and OSIRIS, Atmos. Chem. Phys., 14, 3479–3496, doi:10.5194/acp-14-3479-2014, 2014. 9953, 9956, 9958

Snow, M., Weber, M., Machol, J., Viereck, R., and Richard, E.: Comparison of Magnesium II core-to-wing ratio observations during solar minimum 23/24, J. Space Weather Space Clim., 4, A04, doi:10.1051/swsc/2014001, 2014. 9956

Solomon, S., Kiehl, J. T., Garcia, R. R., and Grose, W.: Tracer transport by the diabatic circulation deduced from satellite-observations, J. Atmos. Sci., 43, 1603–1617, doi:10.1175/1520-0469(1986)043<1603:TTBTDC>2.0.CO;2, 1986. 9960

Sonkaew, T., Rozanov, V. V., von Savigny, C., Rozanov, A., Bovensmann, H., and Burrows, J. P.: Cloud sensitivity studies for stratospheric and lower mesospheric ozone profile retrievals from measurements of limb-scattered solar radiation, Atmos. Meas. Tech., 2, 653–678, doi:10.5194/amt-2-653-2009, 2009. 9954

Stiller, G. P., von Clarmann, T., Haenel, F., Funke, B., Glatthor, N., Grabowski, U., Kellmann, S., Kiefer, M., Linden, A., Lossow, S., and López-Puertas, M.: Observed temporal evolution of global mean age of stratospheric air for the 2002 to 2010 period, Atmos. Chem. Phys., 12, 3311–3331, doi:10.5194/acp-12-3311-2012, 2012. 9953, 9959

Thompson, A. M., Witte, J. C., McPeters, R. D., Oltmans, S. J., Schmidlin, F. J., Logan, J. A., Fujiwara, M., Kirchhoff, V. W. J. H., Posny, F., Coetzee, G. J. R., Hoegger, B., Kawakami, S., Ogawa, T., Johnson, B. J., Vömel, H., and Labow, G.: Southern Hemisphere Additional Ozonesondes (SHADOZ) 1998–2000 tropical ozone climatology – 1. Comparison with Total Ozone Mapping Spectrometer (TOMS) and ground-based measurements, J. Geophys. Res.-Atmos., 108, 8238, doi:10.1029/2001JD000967, 2003. 9954

Thompson, A. M., Miller, S. K., Tilmes, S., Kollonige, D. W., Witte, J. C., Oltmans, S. J., Johnson, B. J., Fujiwara, M., Schmidlin, F. J., Coetzee, G. J. R., Komala, N., Maata, M., Mohamad, M. B., Nguyo, J., Mutai, C., Ogino, S.-Y., Da Silva, F. R., Paes Leme, N. M., Posny, F., Scheele, R., Selkirk, H. B., Shiotani, M., Stuebi, R., Levrat, G., Calpini, B., Thouret, V., Tsuruta, H., Valverde Canossa, J., Voemel, H., Yonemura, S., Andres Diaz, J., Thanh, N. T. T., and Ha, H. T. T.: Southern Hemisphere Additional Ozonesondes (SHADOZ) ozone climatology (2005–2009): tropospheric and Tropical Tropopause Layer (TTL) profiles with comparisons to OMI-based ozone products, J. Geophys. Res.-Atmos., 117, D23301, doi:10.1029/2011JD016911, 2012. 9954

Thompson, D. and Solomon, S.: Recent stratospheric climate trends as evidenced in radiosonde data: global structure and tropospheric linkages, J. Climate, 18, 4785–4795, doi:10.1175/JCLI3585.1, 2005. 9952

Wang, H., Cunnold, D., Thomason, L., Zawodny, J., and Bodeker, G.: Assessment of SAGE version 6.1 ozone data quality, J. Geophys. Res.-Atmos., 107, 4691, doi:10.1029/2002JD002418, 2002. 9954

ACPD

14, 9951–9973, 2014

Title Page

Abstract | Introduction

Conclusions | References

Tables | Figures

◂◂ | ▸▸

◂ | ▸

Back | Close

Full Screen / Esc

Printer-friendly Version

Interactive Discussion

Waugh, D. W., Oman, L., Kawa, S. R., Stolarski, R. S., Pawson, S., Douglass, A. R., Newman, P. A., and Nielsen, J. E.: Impacts of climate change on stratospheric ozone recovery, Geophys. Res. Lett., 36, L03805, doi:10.1029/2008GL036223, 2009. 9952, 9953, 9959

Wolter, K. and Timlin, M. S.: El Nino/Southern Oscillation behaviour since 1871 as diagnosed in an extended multivariate ENSO index (MEI.ext), Int. J. Climatol., 31, 1074–1087, doi:10.1002/joc.2336, 2011. 9956

World Meteorological Organization: Scientific Assessment of Ozone Depletion: 2010, Global Ozone Research and Monitoring Project-Report No. 52, Geneva, Switzerland, 2011. 9959

Young, P. J., Rosenlof, K. H., Solomon, S., Sherwood, S. C., Fu, Q., and Lamarque, J.-F.: Changes in stratospheric temperatures and their implications for changes in the Brewer–Dobson circulation, 1979–2005, J. Climate, 25, 1759–1772, doi:10.1175/2011JCLI4048.1, 2012. 9952

ACPD

14, 9951–9973, 2014

Hiatus in the acceleration of tropical upwelling

J. Aschmann et al.

Table 1. Geolocation, temporal coverage and average LS O_3 column of utilised SHADOZ sites.

Name	Location		Coverage	Average [DU]
Ascension Is.	14.4° W	8.0° S	Jan 1998–Aug 2010	28.76
Costa Rica	84.0° W	9.9° N	Jul 2005–Dec 2012	30.66
Hilo	155.0° W	19.4° N	Jan 1998–Feb 2013	36.97
Watukosek-Java	112.6° E	7.5° S	Jan 1998–Jun 2013	27.06
Kuala Lumpur	101.7° E	2.7° N	Jan 1998–Dec 2011	30.26
Nairobi	36.8° E	1.3° S	Jan 1998–Jun 2013	30.66
Natal	35.3° W	5.5° S	Jan 1998–May 2011	29.74
Paramaribo	55.2° W	5.8° N	Sep 1999–Dec 2011	31.53
Samoa	170.6° W	14.2° S	Jan 1998–Dec 2012	30.91
San Cristobal	89.6° W	0.9° S	Mar 1998–Oct 2008	29.26

ACPD
14, 9951–9973, 2014

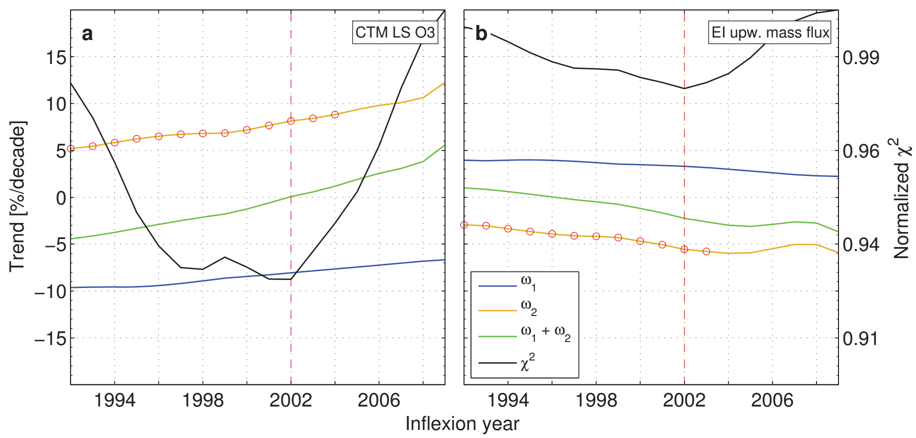

Fig. 1. The dependence of the linear fit parameters ϖ_1, ϖ_2 and ϖ ($\varpi_1 + \varpi_2$) on the inflexion year T_0 is shown for the regression of modelled tropical LS O_3 column **(a)** and EI upward mass flux at 70 hPa **(b)**. Red circles denote the years where the trend-change (ϖ_2) exceeds the 95 % confidence threshold. The black lines are the normalised χ^2 values of the fit residuals.

ACPD
14, 9951–9973, 2014

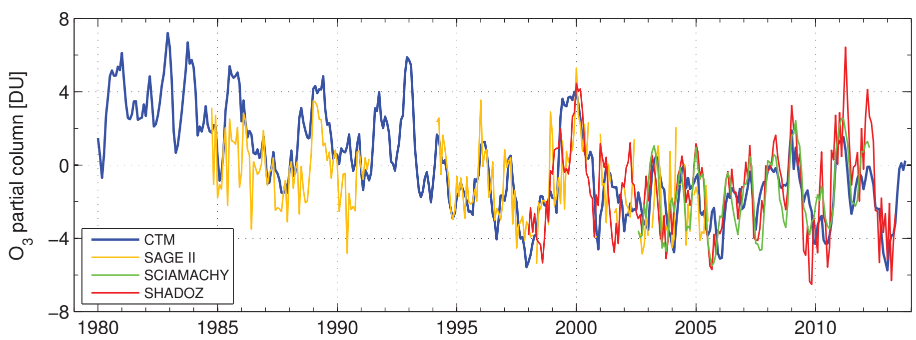

Fig. 2. Observed and simulated tropical (20° N–20° S) LS O_3 partial columns (17–21 km). Anomalies are deviations from the modelled 1980–2013 averages.

ACPD
14, 9951–9973, 2014

Hiatus in the acceleration of tropical upwelling

J. Aschmann et al.

Title Page
Abstract Introduction
Conclusions References
Tables Figures
◂ ▸
Back Close
Full Screen / Esc
Printer-friendly Version
Interactive Discussion

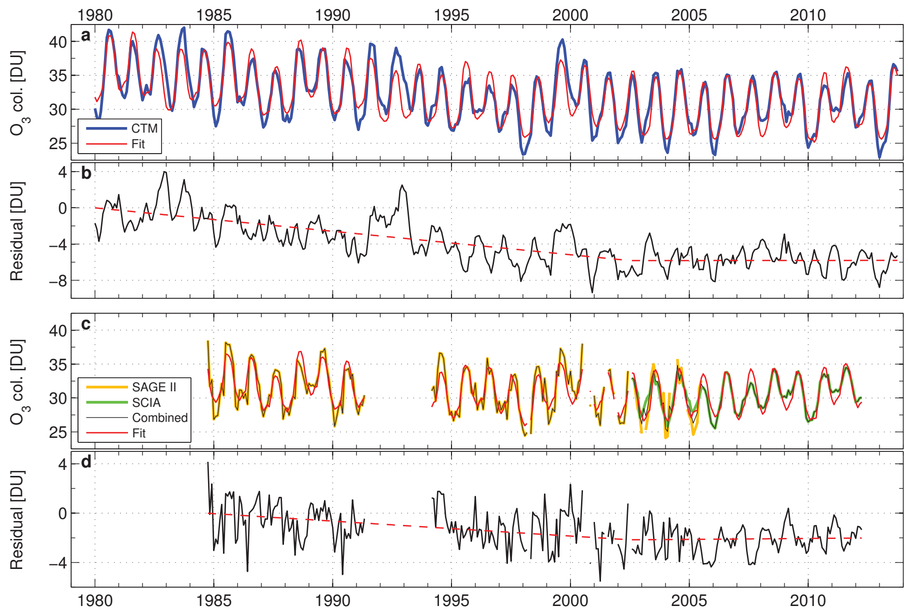

Fig. 3. Regression analysis of observed and simulated O_3 partial columns. Model and combined SAGE II/SCIAMACHY LS O_3 with regression function **(a, c)**. Corresponding fit residuals excluding the linear terms **(b, d)**. The dashed red lines depict the resulting linear trends before and after 2002.

ACPD
14, 9951–9973, 2014

Hiatus in the acceleration of tropical upwelling

J. Aschmann et al.

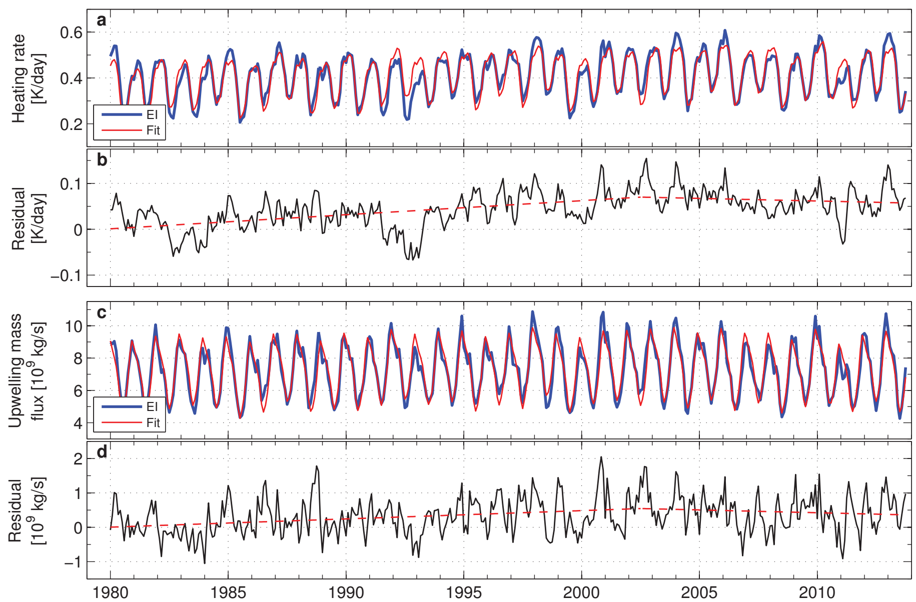

Fig. 4. Regression analysis of EI LS heating rate (17–21 km; **a, b**) and upwelling mass flux (70 hPa; **c, d**). Setup identical to Fig. 3 otherwise.

ACPD
14, 9951–9973, 2014

Hiatus in the acceleration of tropical upwelling

J. Aschmann et al.

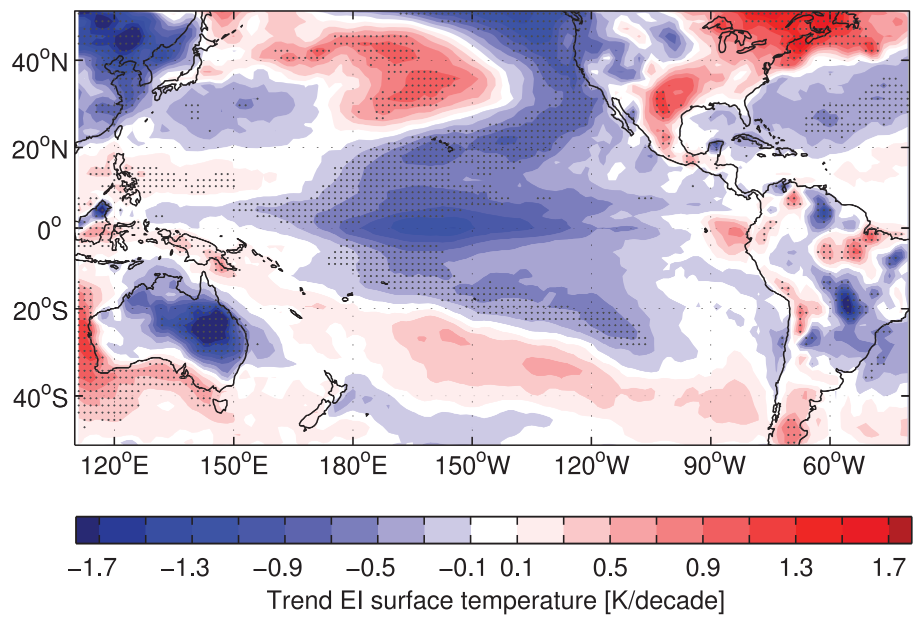

Fig. 5. Linear trends of EI surface temperature from 2002–2013. Stippling indicates where the trend exceeds the 95 % confidence threshold. Setup adapted from Kosaka and Xie (2013).

ACPD
14, 9951–9973, 2014

Hiatus in the acceleration of tropical upwelling

J. Aschmann et al.

Title Page
Abstract | Introduction
Conclusions | References
Tables | Figures
◀| |▶
◀ ▶
Back | Close
Full Screen / Esc
Printer-friendly Version
Interactive Discussion